RSC Advances

REVIEW

View Article Online
View Journal | View Issue

Cite this: *RSC Adv.*, 2025, **15**, 12047

Research progress on structural regulation of nitrogen-fixing photocatalysts

Zhao Zhanfeng, †*[a] Zhang Yue†[b] and Gao Ningning[a]

Photocatalytic nitrogen fixation is a forward-looking technology for zero-carbon nitrogen fixation, which is crucial for alleviating the energy crisis and achieving carbon neutrality. Based on research into the structural regulation of nitrogen-fixing photocatalysts, this review summarizes the latest progress and challenges in photocatalytic ammonia synthesis from three dimensions: active sites, crystal structures, and composite structures. In terms of active site construction, common types of active sites, including metal sites, non-metal sites, vacancies, and single atoms, are discussed. Their characteristics and methods for improving photocatalytic nitrogen fixation performance are analyzed. Furthermore, starting from the mechanism of nitrogen activation, a general strategy for active sites to promote the electron exchange process and thereby enhance nitrogen activation efficiency is explored. In terms of crystal structure construction, the design of nitrogen-fixing photocatalysts is described from three perspectives: crystal form, crystal facet, and morphology control. In terms of composite structure construction, this review discusses the key role of structures such as semiconductor–metal composites and semiconductor–semiconductor composites in promoting carrier separation. It is hoped that this review can provide new insights for the design and preparation of efficient nitrogen-fixing photocatalysts and inspire practical applications of photocatalytic nitrogen fixation.

Received 9th February 2025
Accepted 10th April 2025

DOI: 10.1039/d5ra00953g

rsc.li/rsc-advances

1. Introduction

Nitrogen fixation, the conversion of free nitrogen molecules (*e.g.*, N_2) into nitrogen compounds absorbable by humans for synthesizing essential substances such as DNA, RNA, and proteins, serves as a crucial cornerstone in maintaining ecological cycles in nature.[1,2] NH_3, the primary product of nitrogen fixation, is not only a vital raw material in manufacturing, widely used in fertilizers, the military, pharmaceuticals, and other fields, but also regarded as an ideal hydrogen storage carrier due to its high energy density (3 kW h kg^{-1}), high hydrogen capacity (17.6 wt%), ease of liquefaction, and convenience in transportation.[3]

Artificial nitrogen fixation dates back to the mid-19th century, but the Haber–Bosch process in 1909 ushered in its modern era.[1] Since NH_3, the main product of industrial nitrogen fixation, is also the primary raw material for fertilizers, the Haber–Bosch process has led to a 400% increase in world

[a]*SINOPEC Research Institute of Petroleum Processing, State Key Laboratory of Petroleum Molecular & Process Engineering, Beijing, China. E-mail: zhaozhanfeng.ripp@sinopec.com*

[b]*China Wuzhou Engineering Group Corporation Ltd, First Design and Research Institute, Beijing, China*

† Zhao Zhanfeng and Zhang Yue contributed equally to the work.

Zhao Zhanfeng

Zhao Zhanfeng, born in May 1993, obtained his PhD from Tianjin University in 2023. He is currently employed at the Sinopec Research Institute of Petroleum and Petrochemicals, where his primary research focuses on photocatalytic nitrogen fixation and the structural regulation of metal–organic framework materials.

Zhang Yue

Zhang Yue, born in April 1996, obtained her PhD from Tianjin University in 2024. She is currently working at China Wuzhou Engineering Group Corporation Ltd, with her primary research focusing on the structural regulation of catalysts.

food production since its introduction, fundamentally transforming food production methods.[3] However, the Haber–Bosch process requires harsh conditions of high temperature (700 K) and high pressure (100 atm) to catalyze the reaction between N_2 and hydrogen (H_2) to produce NH_3, consuming approximately 2% of the world's total energy and emitting about 3% of global CO_2 annually.[3] In the Haber–Bosch process, about 72% of H_2 is supplied by natural gas-based hydrogen production, and the energy consumption of the H_2 production process accounts for about 75% of the total energy consumption of ammonia synthesis. The high energy consumption of the Haber–Bosch process necessitates the pursuit of greener and more sustainable pathways for artificial nitrogen fixation.

In addition to the thermocatalytic approach represented by the Haber–Bosch process, there are also enzymatic catalysis, electrocatalysis, and photocatalysis that can efficiently fix nitrogen. Microorganisms (such as bacteria) can utilize nitrogenase to reduce N_2 to NH_3. Another direction in microbial nitrogen fixation is the modification of nitrogen-fixing genes into eukaryotic organisms,[4] such as plants, and the use of nitrogen-fixing microorganisms in electrocatalytic devices to continuously reduce N_2 to NH_3. These microbial nitrogen fixation processes help alleviate the demand for NH_3 but are difficult to apply to modern intensive agricultural production.[3] Electrocatalytic technology provides an alternative method to transfer electrons to nitrogenase without ATP hydrolysis, and various electrocatalysts have been developed to directly reduce N_2 to NH_3 under external electrical energy. Since the primary power generation method of China is still thermal power, utilizing renewable energy instead of electrical energy could significantly reduce energy consumption and CO_2 emissions, simultaneously contributing to the goal of achieving carbon neutrality by 2060.

Photocatalytic nitrogen fixation technology, directly driven by solar energy, can catalyze the conversion of N_2 to NH_3 using H_2O instead of H_2 under mild conditions with no carbon emissions, making it a promising forward-looking technology for artificial nitrogen fixation. In 1977, Schrauzer and Guth used titanium dioxide (TiO_2) as a nitrogen fixation catalyst to achieve the reduction of N_2 to produce trace amounts of ammonia under illumination.[5] Since then, photocatalytic nitrogen fixation technology has been receiving widespread attention.

Gao Ningning

Gao Ningning, born in November 1985, obtained her PhD from the Dalian Institute of Chemical Physics, Chinese Academy of Sciences in 2014. She is currently working at Sinopec Research Institute of Petroleum and Petrochemicals Co., Ltd, with her primary research focusing on photocatalysis, industrial catalysis, adsorptive separation, and membrane separation.

Photocatalytic nitrogen fixation technology utilizes photogenerated carriers to achieve the oxidation and reduction of reactants. The main process is illustrated in Fig. 1a.

1.1 Generation of photogenerated carriers

Photocatalysts are generally semiconductors with a valence band filled with electrons and a conduction band devoid of electrons, separated by a forbidden band. When incident light with an energy greater than or equal to the band gap (E_g) illuminates the photocatalyst, electrons in the valence band are excited to the conduction band, leaving holes in the valence band. The E_g value determines the light absorption range of the catalyst, and its maximum absorption wavelength (λ) can be calculated using the empirical formula: $\lambda = 1240/E_g$.

1.2 Separation and transport of photogenerated carriers

The photogenerated electrons and holes produced by light excitation in semiconductor photocatalysts separate from each other and migrate to the surface, but they may rapidly recombine and annihilate within picoseconds, leading to a significant portion of photogenerated carriers being unable to be effectively utilized, which significantly reduces the incident light utilization efficiency of the catalyst.[7] Various strategies have been employed to promote carrier separation, including heterostructure construction,[8] material compositing,[9] and element doping.[10]

1.3 Utilization of photogenerated carriers

The electrons transported to the catalyst surface undergo reduction reactions (N_2 accepts electrons to synthesize NH_3), while the holes undergo oxidation reactions (H_2O provides electrons to synthesize O_2). N_2 molecules are first enriched on the catalyst surface through physical adsorption and then activated by the catalyst, followed by reduction to the product NH_3 through a continuous hydrogenation process.

To achieve efficient photocatalytic nitrogen fixation, an accurate understanding of the properties of N_2 is essential. N_2 is a linear molecule composed of two N atoms linked by a covalent bond (Fig. 1b). According to molecular orbital theory, the 2p orbitals of the two N atoms hybridize to form new bonding orbitals (2σ and π) and antibonding orbitals ($2\sigma^*$ and π^*). The six electrons from the 2p orbitals fill the three bonding orbitals, forming a high-strength N≡N triple bond. Thermodynamically, the N≡N triple bond has a bond energy as high as 941 kJ mol^{-1}, with the dissociation energy of the first bond reaching 410 kJ mol^{-1}, severely hindering the dissociation of N≡N; kinetically, the large energy gap (10.82 eV) of the N_2 molecule obstructs electron transfer; in terms of reactivity, the low proton affinity ($\Delta H^0 = 37.6$ kJ mol^{-1}), low electron affinity (−1.9 eV), and high ionization energy (15.85 eV) indicate that the protonation and activation of N_2 are extremely difficult.[11] Therefore, N_2 is often used as an inert gas, and the N≡N bond is considered one of the most stable chemical bonds. Due to these inherent inert properties of N_2, its utilization poses a significant challenge.

Photocatalytic nitrogen fixation catalysts, as the core of photocatalytic nitrogen fixation technology, are the focus of research

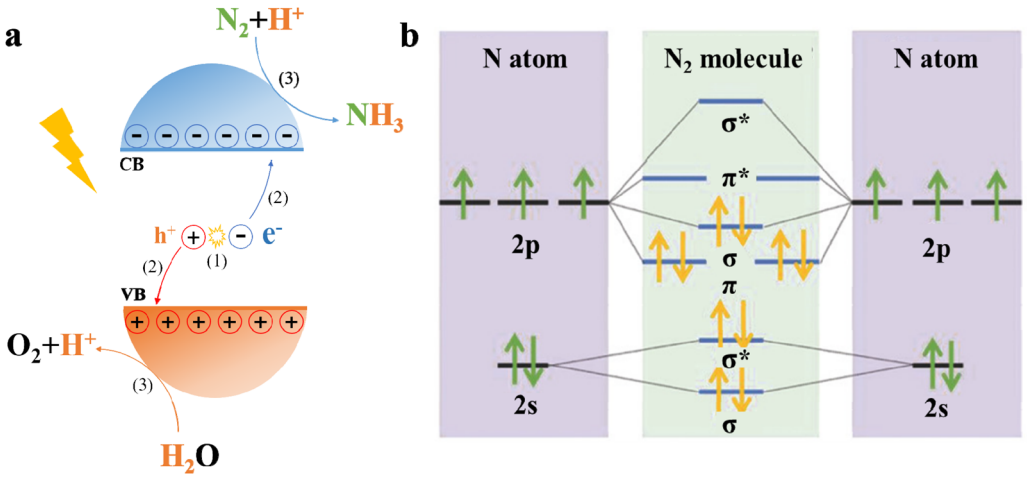

Fig. 1 (a) Schematic diagram of the mechanism of photocatalytic nitrogen fixation; (b) schematic diagram of N atomic orbitals and N_2 molecular hybrid orbitals.[6]

in this field. In recent years, several reviews have been published on nitrogen fixation photocatalyst materials[12] and catalytic mechanisms,[13,14] but there are fewer reviews on catalyst structures, especially structural modulation related directly to catalytic performance, such as active site structure, crystal structure, and composite structure. Therefore, this review aims to summarize the research progress in structural modulation of nitrogen fixation photocatalysts in recent years, focusing on three dimensions: active sites, crystal structure, and composite structure of nitrogen fixation photocatalysts (Fig. 2), and to propose prospects for future development, hoping to further promote the development of the field of photocatalytic nitrogen fixation.

2. Structural construction of photocatalytic nitrogen fixation catalysts

2.1 Construction of active sites

The design and construction of active sites are crucial for achieving efficient photocatalytic nitrogen fixation. Active sites need not only to effectively adsorb N_2 but also to rapidly accept electrons and protons for N_2 reduction. Currently, the performance of nitrogen fixation photocatalysts still lags significantly behind practical production demands. On the one hand, the difficulty in activating N_2 limits the activity of photocatalytic nitrogen fixation. On the other hand, competition from hydrogen evolution reactions constrains the selectivity of photocatalytic nitrogen fixation. The activation mechanism of N_2 is generally accepted as the π-backdonation mechanism proposed by Han *et al.*,[13] which divides N_2 activation into two processes: process 1 involves the empty d-orbitals of the metal accepting electrons from the σ_g bonding orbital of N_2, and process 2 involves the occupied d-orbitals of the metal donating electrons to the π_g^* antibonding orbital of N_2. It can be seen that N_2 activation is essentially an electron exchange process between the active site and the N_2 molecule. Therefore, enhancing the electron exchange between the active site and the N_2 molecule is an effective way to promote N_2 activation. On the one hand, the transfer of electrons from N_2 to the metal can be enhanced by pulling the two lone pairs of electrons at the ends of N_2. Wang *et al.*[15] anchored B atoms on the surface of metal-free black phosphorus materials based on first-principles theoretical calculations, where adjacent B atoms formed "Lewis acid pairs" generating a "pull–pull effect" on N_2 molecules. Simulation calculations showed that the B atoms could attract electrons from the N_2 molecules and transfer them to the B atoms, and the resulting "pull–pull effect" could reduce the activation energy barrier of N_2 and promote N_2 activation to a certain extent. Building on this research, Wang *et al.*[16] further used bimetallic sites instead of monometallic sites to promote the transfer of electrons from N_2 to the metal. They screened FeMo/g-C_3N_4, TiMo/g-C_3N_4, MoW/g-C_3N_4, and NiMo/g-C_3N_4 catalysts among 28 catalyst combinations through theoretical calculations. These four catalysts have suitable bandgap structures and visible light absorption capabilities, making them promising candidates for efficient nitrogen fixation photocatalysts. On the other hand, methods such as constructing heterojunctions[17] and forming localized surface plasmon resonance fields[15] can

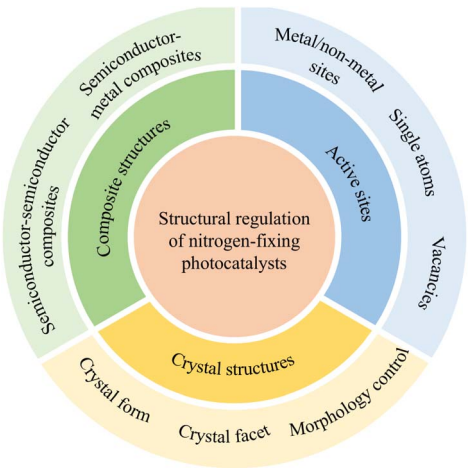

Fig. 2 Structural regulation of nitrogen-fixing photocatalysts.

be used to promote the transfer of electrons from metal to N_2. Huang *et al.*[17] loaded Bi metal cocatalysts on the surface of BiOBr to form a Bi/semiconductor interfacial Schottky junction. The introduction of Bi could not only promote interfacial electron transfer in the photocatalyst but also facilitate N_2 activation due to its strong electron donation. This unidirectional electron transfer from BiOBr to the active site Bi increased the efficiency of photocatalytic ammonia synthesis by 65 times. Bimetallic systems exhibit enhanced nitrogen activation by decoupling the electron acceptance and donation processes. For instance, Zhao *et al.*[18] demonstrated that bimetallic organic frameworks (BMOFs) composed of hard-acid (high ionization potential, I_n) and soft-acid (low I_n) metal nodes synergistically promote N≡N bond cleavage. The hard-acid metal (*e.g.*, Fe) facilitates electron withdrawal from N_2 *via* σ-bond interaction, while the soft-acid metal (*e.g.*, Sr) donates electrons to the π*-antibonding orbitals of N_2. This decoupling strategy reduces the activation energy barrier and enhances electron exchange efficiency, achieving an NH_3-evolution rate of 780 μmol g^{-1} h^{-1} under visible light.

In recent years, constructing coordination unsaturated sites through vacancies has become one of the research hotspots in the field of photocatalytic nitrogen fixation. Vacancies in photocatalysts can not only promote the adsorption of N_2 but also facilitate charge separation to a certain extent. Vacancies are mainly classified into oxygen vacancies, nitrogen vacancies, carbon vacancies, and sulfur vacancies based on the missing elements, with oxygen vacancies being widely used in the field of photocatalytic nitrogen fixation. Shiraishi *et al.*[19] investigated the effect of oxygen vacancies on the photocatalytic nitrogen fixation of TiO_2. They proposed that Ti^{3+} groups formed at the oxygen vacancies on the TiO_2 surface served as active sites that could effectively capture electrons and promote N_2 activation (Fig. 3a). To better create oxygen vacancies, researchers typically choose materials rich in oxygen elements as photocatalysts. Layered double hydroxides (LDH) are increasingly gaining attention due to their controllable electronic structure and low cost. Zhang *et al.*[20] were the first to apply CuCr-LDH nanosheets (CuCr-NS) rich in oxygen vacancies to the field of photocatalytic nitrogen fixation. Under full-spectrum irradiation, the photocatalytic ammonia synthesis rate of CuCr-NS was 78.6 μmol g^{-1} h^{-1}, with an apparent quantum efficiency (AQE) of 2.4% at a wavelength of 400 nm. Subsequently, they optimized the oxygen vacancies by incorporating coordination unsaturated $Cu^{\delta+}$ species onto ZnAl-LDH nanosheets (Fig. 3b).[21] DFT theoretical calculations indicated that the oxygen vacancies and $Cu^{\delta+}$ species could effectively promote N_2 adsorption and activation.

Zhang *et al.*[22] reported BiOBr nanosheets (BOB-001-OV) with oxygen vacancies that could stretch the N≡N bond length from 1.078 Å to 1.133 Å. Theoretical calculations showed that the defect states induced by oxygen vacancies could act as electron acceptors to effectively inhibit electron–hole pair recombination and enhance charge transfer from BOB-001-OV to N_2 molecules. Fluorescence spectroscopy revealed that the average lifetime (τ) of BOB-001-OV was 2.15 ns, approximately twice that of BiOBr without oxygen vacancies, demonstrating that oxygen vacancies could promote the migration of photogenerated carriers. The ammonia synthesis rate of BOB-001-OV under visible light was 104.3 μmol g^{-1} h^{-1}, with an AQE of 0.23% at 420 nm. Simultaneously, the generated O_2 was stoichiometrically close to 75% of produced NH_3, proving that H_2O could serve as an electron donor to achieve a complete chemical cycle in photocatalytic nitrogen fixation.

Single-atom catalysts (SACs) have garnered significant attention due to their rapid electron–hole separation and targeted active sites. The atomic-level dispersion of SACs maximizes atomic utilization and can anchor SACs as active sites to enhance nitrogen fixation activity in the field of photocatalytic nitrogen fixation. Wang *et al.*[23] established a g-C_3N_4 model anchored with single B atoms (B/g-C_3N_4) and simulated the reduction process of N_2 on B/g-C_3N_4 through first-principles calculations (Fig. 4a). The calculation results showed that B/g-C_3N_4 could effectively reduce gaseous N_2 molecules through an

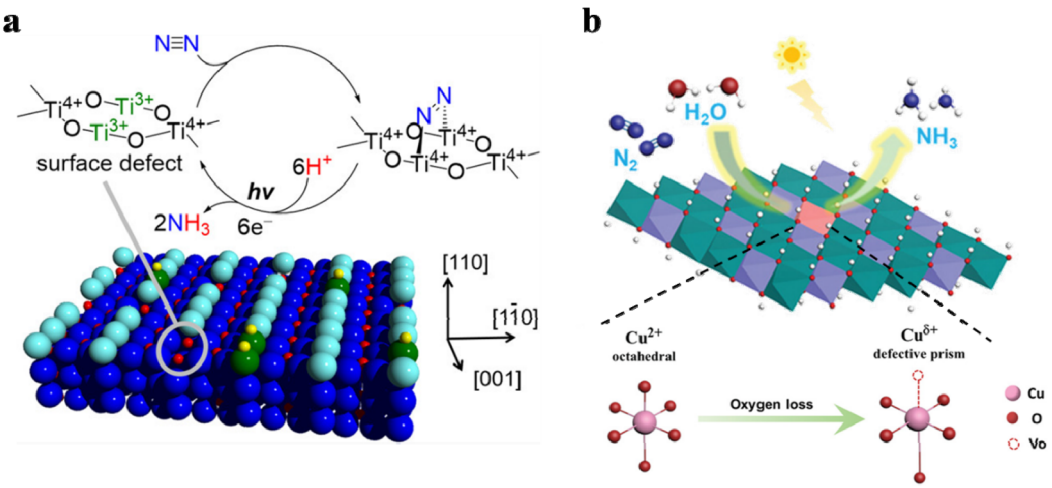

Fig. 3 (a) Schematic diagram of the photocatalytic nitrogen fixation cycle on the oxygen vacancies of TiO_2;[20] (b) schematic diagram of the photocatalytic nitrogen fixation process of ZnAl-LDH nanosheets and the formation process of electron-rich $Cu^{\delta+}$ and oxygen vacancies.[21]

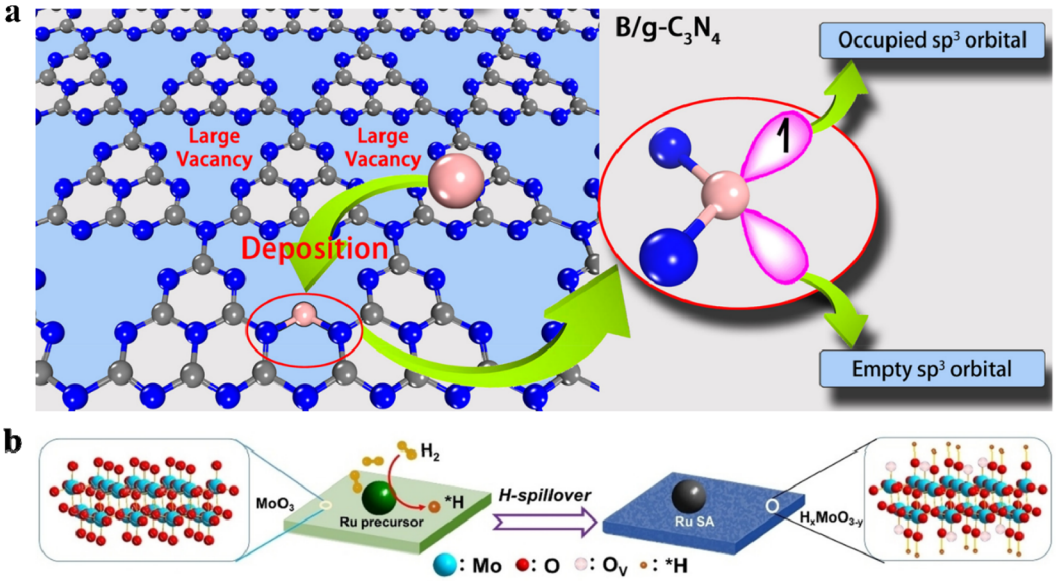

Fig. 4 (a) Design concept of the B/g-C_3N_4 photocatalyst;[23] (b) schematic diagram of the structure and preparation process of the Ru-SA/H_x-MoO_{3-y} photocatalyst.[24]

enzymatic mechanism at an extremely low initial potential. In addition, anchoring single B atoms significantly enhanced the visible and infrared light absorption of g-C_3N_4, granting the catalyst strong N_2 reduction capabilities. To address the issue of insufficient local electron supply. Yin *et al.*[25] prepared the Ru-SA/H_xMoO_{3-y} photocatalyst by combining Ru single atoms (Ru-SA) with molybdenum oxide rich in oxygen vacancies and conducted photocatalytic nitrogen fixation studies using N_2 and H_2 as reactants (Fig. 4b). Ru-SA facilitated the activation of N_2 molecules and the migration of H_2 molecules, while Mo sites containing oxygen vacancies captured local electrons and catalyzed the reduction of N_2 molecules, ultimately achieving an ammonia synthesis rate of 4 mmol g^{-1} h^{-1} for SA/H_xMoO_{3-y}.

2.2 Crystal structure construction

Research on the regulation of the crystal structure of photocatalysts for photocatalytic nitrogen fixation primarily focuses on crystal form, crystal facet and morphology control. Semiconductor photocatalysts are mostly crystalline materials, and their orderly crystal structure facilitates electron transfer and reduces the recombination of photogenerated carriers. Crystal form is a fundamental characteristic of crystalline materials, and research into the crystal form of nitrogen fixation photocatalysts can be traced back to the inception of photocatalytic nitrogen fixation. In 1977, Schrauzer *et al.*[5] found that after calcination at 1000 °C, some TiO_2 impregnated with iron sulfate could transform from the anatase phase to the rutile phase, achieving the highest photocatalytic nitrogen fixation activity when the loading of Fe_2O_3 reached 0.2%. Active site density is one of the critical factors directly affecting photocatalytic efficiency. Overly ordered crystal structures cannot expose sufficient active sites for N_2 adsorption, thereby hindering the adsorption and activation of N_2 molecules on the active sites to some extent. Hou *et al.*[24] prepared amorphous SmOCl nanosheet materials using graphene oxide as a template. With increasing amorphization of the SmOCl nanosheets, numerous oxygen vacancies formed on the surface of the nanosheets, significantly promoting the adsorption and activation of N_2 molecules. Additionally, the authors observed enhanced Sm–O covalent bonds, indicating electron migration from bulk to surface for combination with N_2. Under illumination, the ammonia synthesis rate of SmOCl nanosheets reached 426 μmol g^{-1} h^{-1}, with an AQE of 0.32% at 420 nm.

By precisely and rationally exposing specific crystal facets, the crystals with target facets can be controlled at the atomic scale. The atomic distribution on the crystal facets also significantly influences the active sites and electronic structure of photocatalysts, prompting an increasing number of researchers to attempt to enhance photocatalytic nitrogen fixation activity by regulating the crystal facets of semiconductors. Atoms arrange differently on different exposed facets, hence facet regulation can significantly impact the enhancement of photocatalytic nitrogen fixation activity. Bai *et al.*[27] prepared two types of Bi_5O_7I nanosheets exposing the (100) and (001) facets through hydrolysis and calcination methods. Further experiments demonstrated that the conduction band potential of Bi_5O_7I-001 (−1.45 V) was more negative than that of Bi_5O_7I-100 (−0.85 V), and Bi_5O_7I-001 exhibited higher photogenerated carrier separation efficiency and photocatalytic ammonia synthesis activity. When using ethanol as a hole scavenger, the photocatalytic ammonia synthesis rate of Bi_5O_7I-001 reached 111.5 μmol g^{-1} h^{-1}. Li *et al.*[26] systematically investigated the influence of the (001) and (010) facets of BiOCl nanosheets on the adsorption and activation of N_2 (Fig. 5a). Experimental results showed that N_2 molecules primarily bind through a terminal pathway on (001) facet of BiOCl (Fig. 5b), whereas

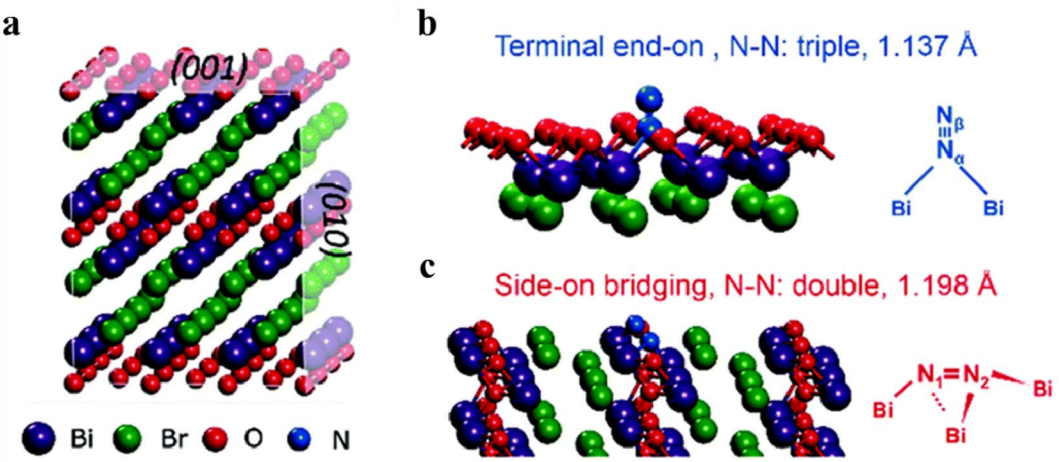

Fig. 5 (a) Crystal structure of BiOCl and corresponding (001) and (010) crystal facets; (b) N_2 molecules bind to the (001) crystal facet of BiOCl through a terminal pathway; (c) N_2 molecules bind to the (010) crystal facet of BiOCl through a side-on bridging pathway.[26]

they primarily bind through a side-on bridging pathway on (010) facet (Fig. 5c). The photocatalytic ammonia synthesis rate of (010) facet of BiOCl was approximately 2.5 times higher than that of (001) facet, reaching 4.62 μmol g^{-1} h^{-1}. Zhang *et al.*[28] combined facet regulation with defect regulation by constructing defects on the (040) facet of $BiVO_4$ single crystals, which induced V^{4+}/V^{5+} sites. Among them, V^{4+} sites are responsible for the chemical adsorption of N_2, while V^{5+} sites serve as bridges for electron transfer, delivering electrons captured by defects to V^{4+} sites for NH_3 synthesis. In contrast, the (110) facet of $BiVO_4$ only contains V^{5+} sites. Therefore, the authors regulated the ratio of (040)/(110) facets by changing the pH during catalyst preparation, achieving a photocatalytic ammonia synthesis rate of 103.4 μmol g^{-1} h^{-1}.

Controllably regulating the morphology of materials is also an effective strategy for crystal regulation, such as one-dimensional nanowires/nanofibers/nanorods, two-dimensional ultrathin nanosheets, and three-dimensional porous/hollow structures. One-dimensional nanostructures can provide direct electron transfer channels, facilitate photogenerated electron transfer, and possess a large specific surface area, providing sufficient active sites for N_2 adsorption. Sun *et al.*[29] applied Nb_2O_5 nanofibers to the field of nitrogen fixation, benefiting from rapid electron exchange and transfer between Nb atoms and N_2 molecules, which led to rapid polarization and activation of adsorbed N_2 molecules. Compared to one-dimensional materials, ultrathin two-dimensional nanosheets feature large lateral dimensions and specific surface areas, which are highly advantageous for the adsorption of N_2 molecules on the surface of photocatalyst. Meanwhile, the high exposure of atoms on two-dimensional nanosheet surfaces suits them for surface modification and functionalization. This includes element doping and vacancy creation, enhancing N_2 adsorption and activation on the catalyst. Cao *et al.*[30] constructed a MXene-Based 2D/2D Ti_3C_2/TiO_2 heterojunction with spatially separated redox sites for photocatalytic N_2 reduction reaction. Electron-rich unsaturated Ti sites on Ti_3C_2 MXene are instrumental in adsorption and activation of N_2, exhibiting a high NH_3 production rate of 24.4 μmol g^{-1} h^{-1}. Three-dimensional materials integrate and optimize the structural advantages of two-dimensional materials. For example, porosity allows rapid transport of N_2 molecules and protons, while hollow structures can utilize internal cavities to reflect and refract incident light for multiple utilizations. Furthermore, three-dimensional flower-like nanospheres assembled from two-dimensional nanosheets combine the advantages of both two-dimensional and three-dimensional materials, potentially boosting light absorption and N_2 adsorption synergistically. Zhang *et al.*[31] reported that Ru-decorated MoO_{3-x} microspheres exhibit dynamic oxygen vacancies which cycle between N_2 adsorption (Ru/MoO_{3-x}) and NH_3 desorption ($Ru/MoO_{3-x}N_y$) states. This H*-mediated oxygen vacancies evolution strategy achieved an NH_3 production rate of 192.38 μmol g^{-1} h^{-1}, 2.68-fold higher than that of pristine MoO_{3-x}. The three-dimensional framework promotes light scattering and provides interconnected pathways for charge transport, addressing the limitations of 2D materials in carrier recombination. However, two-dimensional materials and three-dimensional materials still exist several limitations. Two-dimensional materials (such as ultra-thin nanosheets) present structural instability due to high surface energy, and excessive lateral size may hinder mass transfer. Although three-dimensional porous materials can optimize light absorption, their complex synthesis process limits their large-scale application.[32]

2.3 Construction of composite structures

Composite catalysts are comprised of multiple components. Compared to single structures, their composite structures can better overcome the inherent shortcomings of each component. Even more, the interplay between components may create synergistic effects, achieving a "1 + 1 > 2" outcome. Heterostructures are typical composite structures that regulate photoelectric properties by combining two semiconductor

materials with different band-gap structures. Ghosh *et al.*[33] embedded Bi_2MoO_6 into g-C_3N_4 nanosheets to obtain a g-C_3N_4/Bi_2MoO_6 heterojunction, which exhibited efficient photogenerated carrier separation and N_2 reduction capabilities. Liu *et al.*[10] used TiO_2@C combined with g-C_3N_4 to obtain the TiO_2@C/g-C_3N_4 composite catalyst. Compared to bulk g-C_3N_4, the steady-state photoluminescence spectrum peak intensity of TiO_2@C/g-C_3N_4 significantly decreased. Additionally, the transient photocurrent intensity of TiO_2@C/g-C_3N_4 was approximately 1.7 times higher than that of bulk g-C_3N_4, further proving the positive effect of composite structures on promoting carrier separation. When the molar ratio of TiO_2@C to g-C_3N_4 was 10 : 1, the photocatalytic ammonia synthesis rate of TiO_2@C/g-C_3N_4 reached 250.6 μmol g^{-1} h^{-1}. Xia *et al.*[34] utilized the intrinsic electric field differences between Bi_2O_3 and CoAl-LDH to construct Bi_2O_3@CoAl-LDHs core–shell heterojunction photocatalysts for nitrogen fixation. Hollow Bi_2O_3 microspheres were first prepared using a solvothermal method and then mixed with the precursor solution of CoAl-LDH for a secondary solvothermal reaction to obtain the core–shell composite Bi_2O_3@CoAl-LDHs (Fig. 6). This composite structure photocatalyst had a large interface contact area, effectively promoting carrier separation and achieving a photocatalytic ammonia synthesis rate of 48.7 μmol g^{-1} h^{-1}.

Apart from compositing with semiconductor materials, metal compositing is also a common strategy to promote photogenerated electron–hole separation. In particular, noble metal loading can form Schottky barriers with semiconductors. The resulting energy band bending can effectively inhibit the recombination of photogenerated carriers. Ranjit *et al.*[35] loaded Ru, Rh, Pd, and Pt onto TiO_2 for photocatalytic nitrogen fixation. The authors found that the photocatalytic activity of metal-loaded TiO_2, in descending order, was: Ru > Rh > Pd > Pt. The highest performance was observed for Ru-loaded TiO_2 due to its higher Ru–H bond strength. Ye *et al.*[36] prepared the Ni_2P/$Cd_{0.5}Zn_{0.5}S$ composite photocatalyst by loading transition metal phosphide Ni_2P onto $Cd_{0.5}Zn_{0.5}S$. The authors demonstrated through time-resolved PL spectroscopy, photocurrent, and electrochemical impedance spectroscopy that Ni_2P/$Cd_{0.5}Zn_{0.5}S$ had higher photogenerated electron–hole separation efficiency compared to Ni_2P and $Cd_{0.5}Zn_{0.5}S$. Maimaitizi *et al.*[37] synthesized flower-like N-MoS_2 microspheres through a one-step solvothermal method and then prepared Pt/N-MoS_2 photocatalysts *via* a photo-ultrasonic reduction method. The special multi-level flower-like structure of Pt/N-MoS_2 could provide more active sites. N doping could narrow the bandgap of MoS_2, enhancing its response to visible light. Pt nanoparticles could act as electron traps, forming Schottky barriers, thereby improving photogenerated carrier separation efficiency. They demonstrated that the nitrogen fixation activity of ultrasonic photocatalysis was higher than that of ultrasonic catalysis and photocatalysis, indicating a synergistic effect between ultrasound and visible light irradiation. Schrauzer *et al.*[5] studied the impact of Fe, Cr, Co, and Mo metals on the photocatalytic nitrogen fixation performance of TiO_2. They found that Fe metal significantly enhanced the photocatalytic nitrogen fixation activity. Based on this, Zhao *et al.*[38] further investigated the effect of Fe loading on TiO_2 photocatalytic nitrogen fixation and found that an appropriate concentration of Fe^{3+} could act as a hole trapping site to inhibit the recombination of photogenerated carriers, thereby enhancing photocatalytic activity. Liu *et al.*[39] also reported on Fe-loaded $SrMoO_4$ photocatalysts for nitrogen fixation reactions. They found that as the Fe loading increased from 0 to 5.1%, the bandgap of $SrMoO_4$ decreased from 3.98 eV to 2.93 eV. The bandgap directly affects the light absorption range, so the reduction in band-gap expanded the light absorption range of $SrMoO_4$ from the UV region to the visible region. Additionally, Fe loading could induce surface defects, which could serve as N_2 adsorption sites and inhibit electron–hole pair recombination, thereby effectively enhancing the photocatalytic nitrogen fixation efficiency. Compared to single-metal loading, bimetals may exhibit more effective synergistic effects during photocatalytic nitrogen fixation. Li *et al.*[40] loaded Pt-doped Fe nanoclusters onto g-C_3N_4. This study showed that Pt–Fe nanoclusters could cause upward bending of the semiconductor energy band and form a large Schottky barrier, thereby enhancing the separation of photogenerated carriers and N_2 reduction. Therefore, the FePt@C_3N_4 photocatalyst exhibited an ammonia synthesis rate of 3.7 μmol g^{-1} h^{-1} under visible light irradiation. In addition to photocatalytic nitrogen fixation performance, structural regulation may also impact other properties of the catalyst. Zhang *et al.*[41] demonstrated that introducing oxygen vacancies into Ru/$W_{18}O_{49}$ significantly enhanced the hydrogen spillover effect, which not only improved ammonia synthesis activity but also optimized the hydrogen adsorption/desorption thermodynamics and charge separation efficiency. Specifically, the Schottky junction formed between Ru and $W_{18}O_{49}$ promoted

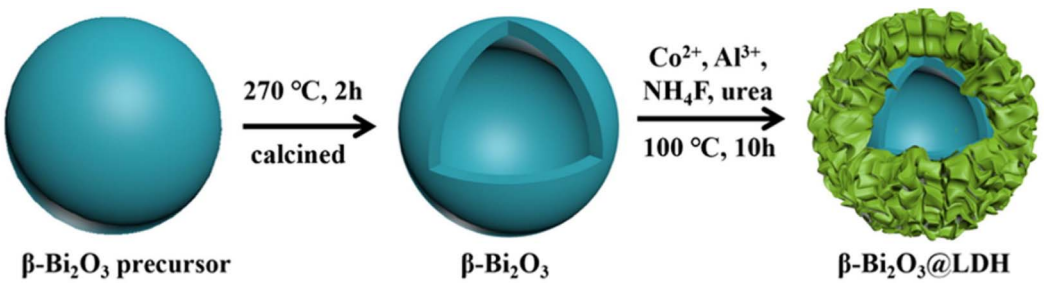

Fig. 6 Schematic diagram of the preparation route of Bi_2O_3@CoAl-LDHs.[34]

electron trapping at Ru sites, reducing recombination losses. Additionally, the OVs-rich structure improved long-term stability, retaining 87% activity after six cycles, highlighting the dual role of structural defects in enhancing both efficiency and durability.

3. Summary and outlook

Photocatalytic nitrogen fixation, as a green and sustainable new process for ammonia synthesis, holds broad application prospects. This paper first briefly introduces the basic principles and existing issues of photocatalytic nitrogen fixation, followed by a review focusing on three dimensions of active site, crystal structure, and composite structure construction in nitrogen fixation photocatalysts. In terms of active site construction, active site design can be approached from the mechanism of photocatalytic nitrogen fixation, strengthening the electron exchange process in nitrogen activation, thereby enhancing the efficiency of photocatalytic nitrogen fixation. Additionally, holes and single atoms are also important research directions. In terms of crystal structure construction, current research primarily focuses on crystal polymorphism, crystal facet, and morphology regulation. High-performance crystal facets can be specifically exposed to enhance activity. Meanwhile, special morphologies such as flower-sphere, hollow microspheres, and core–shell structures are conducive to the reflection and refraction of incident light, increasing the utilization efficiency of incident light. In composite structure construction, both Schottky barriers formed by semiconductor–metal combinations and heterojunctions formed by semiconductor–semiconductor combinations promote photogenerated carrier separation, yielding synergistic effects for "1 + 1 > 2" outcomes. Finally, based on the current research progress in the field of photocatalytic nitrogen fixation, this paper provides an outlook for the field, hoping to promote its development:

(1) Rational design of ternary transfer channels for molecules, protons, and electrons. Photocatalytic nitrogen fixation is a typical complex reaction requiring the simultaneous participation of N_2 molecules, protons, and electrons. The transfer paths, transfer rates, and transfer mechanisms for these three differ. N_2 molecules primarily diffuse with the aqueous solution, protons primarily transfer along the catalyst surface, and electrons primarily transfer along the catalyst framework. Direct contact between protons and electrons may lead to hydrogen evolution reactions. The design of respective transfer channels for molecules, protons, and electrons must ensure rapid material transfer while maintaining independence between channels, posing significant challenges for the structural design of photocatalysts.

(2) Exploration of new mechanisms for photocatalytic nitrogen fixation. Although the photocatalysts prepared in existing research have achieved high activity and selectivity, there is still a significant gap compared to biological nitrogenase. The rich species diversity in nature encompasses various efficient synergistic mechanisms, such as confinement effects, channel effects, compartmentalization effects, and proximity effects. If we can learn from natural coordination mechanisms and reveal new mechanisms for photocatalytic nitrogen fixation using interdisciplinary approaches such as materials genomics and artificial intelligence, it will bring new developments to this field.

(3) Expansion of photocatalyst applications. Photocatalytic nitrogen fixation reactions utilize photogenerated electrons to reduce N_2 molecules. To facilitate the analysis of the catalytic process, hole scavengers are often used to consume photogenerated holes. However, photogenerated holes possess strong oxidizing capabilities. If holes can be utilized to catalyze oxidation to produce higher-value chemicals, it will further broaden the application prospects of photocatalytic technology. Additionally, the stability test time for photocatalysts is generally within 24 hours, and the photocatalytic ammonia synthesis rate is generally at the micromolar level, still far from practical application requirements. Developing catalytic materials and optimizing structural parameters will be key factors in expanding the application of photocatalytic nitrogen fixation.

Data availability

No primary research results, software or code have been included and no new data were generated or analysed as part of this review.

Conflicts of interest

There are no conflicts of interest to declare.

References

1 A. J. Medford and M. C. Hatzell, Photon-driven nitrogen fixation: Current progress, thermodynamic considerations, and future outlook, *ACS Catal.*, 2017, **7**, 2624–2643.
2 A. Chen and B. Y. Xia, Ambient dinitrogen electrocatalytic reduction for ammonia synthesis, *J. Mater. Chem. A*, 2019, **7**, 23416–23431.
3 J. G. Chen, R. M. Crooks, L. C. Seefeldt, K. L. Bren, R. M. Bullock, M. Y. Darensbourg, P. L. Holland, B. Hoffman, M. J. Janik, A. K. Jones, M. G. Kanatzidis, P. King, K. M. Lancaster, S. V. Lymar, P. Pfromm, W. F. Schneider and R. R. Schrock, Beyond fossil fuel-driven nitrogen transformations, *Science*, 2018, **360**, eaar6611.
4 E. J. Vicente and D. R. Dean, Keeping the nitrogen-fixation dream alive, *Proc. Natl. Acad. Sci. U. S. A.*, 2017, **114**, 3009–3011.
5 G. N. Schrauzer and T. D. Guth, Photolysis of water and photoreduction of nitrogen on titanium dioxide, *J. Am. Chem. Soc.*, 1977, **99**, 7189–7193.
6 S. Y. Wang, F. Ichihara, H. Pang, H. Chen and J. H. Ye, Nitrogen fixation reaction derived from nanostructured catalytic materials, *Adv. Funct. Mater.*, 2018, **28**, 1803309.
7 J. Schneider, M. Matsuoka, M. Takeuchi, J. Zhang, Y. Horiuchi, M. Anpo and D. W. Bahnemann, Understanding TiO_2 photocatalysis: Mechanisms and materials, *Chem. Rev.*, 2014, **114**, 9919–9986.

8 Y. Han, X. Lu, S. Tang, X. Yin, Z. Wei and T. Lu, Metal-free 2D/2D heterojunction of graphitic carbon nitride/graphdiyne for improving the hole mobility of graphitic carbon nitride, *Adv. Energy Mater.*, 2018, **8**, 1702992.

9 H. Liang, J. Li and Y. Tian, Construction of full-spectrum-driven Ag-g-C_3N_4/$W_{18}O_{49}$ heterojunction catalyst with outstanding N_2 photofixation ability, *RSC Adv.*, 2017, **7**, 42997–43004.

10 Q. X. Liu, L. H. Ai and J. Jiang, MXene-derived TiO_2@C/g-C_3N_4 heterojunctions for highly efficient nitrogen photofixation, *J. Mater. Chem. A*, 2018, **6**, 4102–4110.

11 X. Chen, N. Li, Z. Kong, W.-J. Ong and X. Zhao, Photocatalytic fixation of nitrogen to ammonia: State-of-the-art advancements and future prospects, *Mater. Horiz.*, 2018, **5**, 9–27.

12 S. Lin, X. Zhang, L. Chen, Q. Zhang, L. Ma and J. Liu, A review on catalysts for electrocatalytic and photocatalytic reduction of N2 to ammonia, *Green Chem.*, 2022, **24**, 9003–9026.

13 Q. Han, H. Jiao, L. Xiong and J. Tang, Progress and challenges in photocatalytic ammonia synthesis, *Mater. Adv.*, 2021, **2**, 564–581.

14 P. Praus, Photocatalytic Nitrogen Fixation using Graphitic Carbon Nitride: A Review, *ChemistrySelect*, 2023, **8**, e202204511.

15 L. Shi, Q. Li, C. Ling, Y. Zhang, Y. Ouyang, X. Bai and J. Wang, Metal-free electrocatalyst for reducing nitrogen to ammonia using a Lewis acid pair, *J. Mater. Chem. A*, 2019, **7**, 4865–4871.

16 S. Y. Wang, L. Shi, X. W. Bai, Q. Li, C. Y. Ling and J. L. Wang, Highly efficient photo-/electrocatalytic reduction of nitrogen into ammonia by dual-metal sites, *ACS Cent. Sci.*, 2020, **6**, 1762–1771.

17 Y. Huang, Y. Zhu, S. Chen, X. Xie, Z. Wu and N. Zhang, Schottky junctions with Bi cocatalyst for taming aqueous phase N_2 reduction toward enhanced solar ammonia production, *Adv. Sci.*, 2021, **8**, 2003626.

18 Z. Zhao, H. Ren, D. Yang, Y. Han, J. Shi, K. An, Y. Chen, Y. Shi, W. Wang, J. Tan, X. Xin, Y. Zhang and Z. Jiang, Boosting nitrogen activation *via* bimetallic organic frameworks for photocatalytic ammonia synthesis, *ACS Catal.*, 2021, **11**, 9986–9995.

19 H. Hirakawa, M. Hashimoto, Y. Shiraishi and T. Hirai, Photocatalytic conversion of nitrogen to ammonia with water on surface oxygen vacancies of titanium dioxide, *J. Am. Chem. Soc.*, 2017, **139**, 10929–10936.

20 Y. Zhao, X. Jia, G. I. N. Waterhouse, L. Wu, C. Tung, D. O'hare and T. Zhang, Layered double hydroxide nanostructured photocatalysts for renewable energy production, *Adv. Energy Mater.*, 2016, **6**, 1501974.

21 S. Zhang, Y. Zhao, R. Shi, C. Zhou, G. I. N. Waterhouse, L. Wu, C.-H. Tung and T. Zhang, Efficient photocatalytic nitrogen fixation over $Cu^{\delta+}$-modified defective ZnAl-layered double hydroxide nanosheets, *Adv. Energy Mater.*, 2020, **10**, 1901973.

22 H. Li, J. Shang, Z. Ai and L. Zhang, Efficient visible light nitrogen fixation with BiOBr nanosheets of oxygen vacancies on the exposed {001} facets, *J. Am. Chem. Soc.*, 2015, **137**, 6393–6399.

23 C. Ling, X. Niu, Q. Li, A. Du and J. Wang, Metal-free single atom catalyst for N_2 fixation driven by visible light, *J. Am. Chem. Soc.*, 2018, **140**, 14161–14168.

24 H. Yin, Z. Chen, Y. Peng, S. Xiong, Y. Li, H. Yamashita and J. Li, Dual Active Centers Bridged by Oxygen Vacancies of Ruthenium Single-Atom Hybrids Supported on Molybdenum Oxide for Photocatalytic Ammonia Synthesis, *Angew. Chem., Int. Ed.*, 2022, **61**(14), e202114242.

25 H. Yin, Z. Chen, Y. Peng, S. Xiong, Y. Li, H. Yamashita and J. Li, Dual active centers bridged by oxygen vacancies of ruthenium single-atom hybrids supported on molybdenum oxide for photocatalytic ammonia synthesis, *Angew. Chem., Int. Ed.*, 2022, **61**, e202114242.

26 H. Li, J. Shang, J. Shi, K. Zhao and L. Zhang, Facet-dependent solar ammonia synthesis of BiOCl nanosheets *via* a proton-assisted electron transfer pathway, *Nanoscale*, 2016, **8**, 1986–1993.

27 Y. Bai, L. Ye, T. Chen, L. Wang, X. Shi, X. Zhang and D. Chen, Facet-dependent photocatalytic N_2 fixation of bismuth-rich Bi_5O_7I nanosheets, *ACS Appl. Mater. Interfaces*, 2016, **8**, 27661–27668.

28 G. H. Zhang, Y. Meng, B. Xie, Z. M. Ni, H. F. Lu and S. J. Xia, Precise location and regulation of active sites for highly efficient photocatalytic synthesis of ammonia by facet-dependent $BiVO_4$ single crystals, *Appl. Catal., B*, 2021, **296**, 120379.

29 J. Han, Z. Liu, Y. Ma, G. Cui, F. Xie, F. Wang, Y. Wu, S. Gao, Y. Xu and X. Sun, Ambient N_2 fixation to NH_3 at ambient conditions: Using Nb_2O_5 nanofiber as a high-performance electrocatalyst, *Nano Energy*, 2018, **52**, 264–270.

30 C. Cao, J. Li, L. Zhang, Y. Hu, L. Zhang and W. Yang, MXene-Based 2D/2D Ti_3C_2/TiO_2 Heterojunction with Spatially Separated Redox Sites for Efficient Photocatalytic N_2 Reduction towards NH_3, *J. Mater. Sci. Technol.*, 2025, **214**, 180–193.

31 L. Zhang, R. Li, L. Guo, L. Cui, X. Zhang, Y. Wang, Y. Wang, X. Jian, X. Gao, C. Fan, J. Wang and J. Liu, Active Hydrogen-Switchable Dynamic Oxygen Vacancies in MoO_{3-x} upon Ru Nanoparticle Decoration for Boosting Photocatalytic Ammonia Synthesis Performance, *ACS Catal.*, 2024, **14**, 5696–5709.

32 Y. Xia, Y. Xu, X. Yu, K. Chang, H. Gong, X. Fan, X. Meng, X. Huang, T. Wang and J. He, Structural Design and Control of Photocatalytic Nitrogen-Fixing Catalysts, *J. Mater. Chem. A*, 2022, **10**, 17377–17394.

33 V. E. Kermani, H. A. Yangjeh, D. H. Khalilabad and S. Ghosh, Nitrogen photofixation ability of g-C_3N_4 nanosheets/Bi_2MoO_6 heterojunction photocatalyst under visible-light illumination, *J. Colloid Interface Sci.*, 2020, **563**, 81–91.

34 S. Xia, G. Zhang, Z. Gao, Y. Meng, B. Xie, H. Lu and Z. Ni, 3D hollow Bi_2O_3@CoAl-LDHs direct Z-scheme heterostructure for visible-light-driven photocatalytic ammonia synthesis, *J. Colloid Interface Sci.*, 2021, **604**, 798–809.

35 K. T. Ranjit, T. K. Varadarajan and B. Viswanathan, Photocatalytic reduction of dinitrogen to ammonia over

noble-metal-loaded TiO_2, *J. Photochem. Photobiol., A*, 1996, **96**, 181–185.

36 L. Ye, C. Han, Z. Ma, Y. Leng, J. Li, X. Ji, D. Bi, H. Xie and Z. Huang, Niloading on $Cd_{0.5}Zn_{0.5}S$ solid solution for exceptional hotocatalytic nitrogen fixation under visible light, *Chem. Eng. J.*, 2017, **307**, 311–318.

37 H. Maimaitizi, A. Abulizi, T. Zhang, K. Okitsu and J. J. Zhu, Facile photo-ultrasonic assisted synthesis of flower-like Pt/N-MoS_2 microsphere as an efficient sonophotocatalyst for nitrogen fixation, *Ultrason. Sonochem.*, 2020, **63**, 104956.

38 W. Zhao, J. Zhang, X. Zhu, M. Zhang, J. Tang, M. Tan and Y. Wang, Enhanced nitrogen photofixation on Fe-doped TiO_2 with highly exposed (101) facets in the presence of ethanol as scavenger, *Appl. Catal., B*, 2014, **144**, 468–477.

39 J. Luo, X. Bai, Q. Li, X. Yu, C. Li, Z. Wang, W. Wu, Y. Liang, Z. Zhao and H. Liu, Band structure engineering of bioinspired Fe doped $SrMoO_4$ for enhanced photocatalytic nitrogen reduction performance, *Nano Energy*, 2019, **66**, 104187.

40 Z. Li, Z. Gao, B. Li, L. Zhang, R. Fu, Y. Li, X. Mu and L. Li, Fe-Pt nanoclusters modified Mott-Schottky photocatalysts for enhanced ammonia synthesis at ambient conditions, *Appl. Catal., B*, 2020, **262**, 118276.

41 L. Zhang, R. Li, L. Cui, Z. Sun, L. Guo, X. Zhang, Y. Wang, Y. Wang, Z. Yu, T. Lei, X. Jian, X. Gao, C. Fan and J. Liu, Boosting Photocatalytic Ammonia Synthesis Performance Over OVs-Rich Ru/$W_{18}O_{49}$: Insights into The Roles of Oxygen Vacancies in Enhanced Hydrogen Spillover Effect, *Chem. Eng. J.*, 2023, **461**, 141892.